

Article

Effective Removal of Microplastic Particles from Wastewater Using Hydrophobic Bio-Substrates

Kalyani Prasad Bhagwat ¹, Denis Rodrigue ²  and Laura Romero-Zerón ^{1,*}¹ Chemical Engineering Department, University of New Brunswick, Fredericton, NB E3B 5A3, Canada² Department of Chemical Engineering, Université Laval, Quebec, QC G1V 0A6, Canada

* Correspondence: laurarz@unb.ca

Abstract: The rapid increase in soil and water pollution is primarily attributed to anthropogenic factors, notably the mismanagement of post-consumer plastics on a global scale. This exploratory research design evaluated the effectiveness of natural hydrophobic cattail (*Typha Latifolia*) fibres (CFs) as bio-adsorbents of microplastic particles (MPPs) from wastewater. The study investigates how the composition of the adsorption environment affects the adsorption rate. Straightforward batch adsorption tests were conducted to evaluate the “spontaneous” sorption of MPPs onto CFs. Five MPP materials (PVC, PP, LDPE, HDPE, and Nylon 6) were evaluated. Industrial wastewater (PW) and Type II Distilled Water (DW) were employed as adsorption environments. The batch test results show that CFs are effective in removing five MPP materials from DW and PW. However, a higher removal percentage of MPPs was observed in PW, ranging from 89% to 100% for PVC, PP, LDPE, and HDPE, while the adsorption of Nylon 6 increased to 29.9%, a removal increase of 50%. These findings indicate that hydrophobic interactions drive the “spontaneous and instantaneous” adsorption process and that adjusting the adsorption environment can effectively enhance the MPP removal rate. This research highlights the significant role that bio-substrates can play in mitigating environmental pollution, serving as efficient, sustainable, non-toxic, biodegradable, low-cost, and reliable adsorbents for the removal of MPPs from wastewaters.



Citation: Bhagwat, K.P.; Rodrigue, D.; Romero-Zerón, L. Effective Removal of Microplastic Particles from Wastewater Using Hydrophobic Bio-Substrates. *Pollutants* **2024**, *4*, 231–250. <https://doi.org/10.3390/pollutants4020015>

Academic Editors: Giovanni Vinti, Francesca Villa and Vladimiro Andrea Boselli

Received: 28 February 2024

Revised: 19 April 2024

Accepted: 22 April 2024

Published: 6 May 2024



Copyright: © 2024 by the authors. Licensee MDPI, Basel, Switzerland. This article is an open access article distributed under the terms and conditions of the Creative Commons Attribution (CC BY) license (<https://creativecommons.org/licenses/by/4.0/>).

Keywords: natural fibres; bio-adsorbents; bio-substrates; hydrophobic bio-adsorbents; microplastic particles; adsorption; wastewaters; removal; plastic pollution; marine pollution; wastewater treatment plants

1. Introduction

The rapid increase in soil and water pollution is primarily attributed to anthropogenic factors, notably the mismanagement of post-consumer plastics on a global scale. The UN Environment Program has estimated that 75 to 199 million tonnes of plastic is currently found in our oceans [1] (p. 3) [2–5]. Since plastic debris is inherently chemically stable, its chemical degradation would take hundreds of years in the natural environment [1–3,6]. Furthermore, under natural environmental conditions, plastic debris is finely fragmented into micro- and nanoparticles by several factors, including UV-radiation, thermal degradation, mechanical stress, animals, roots, and soil organisms. These fragments may be transported by wind, surface, or groundwater routes to remote regions in land and water bodies [7] (p. 164533(2)) [1,5,8,9]. Micro- and nanoplastic particles are considered “...one of the most important environmental threats to marine ecosystems” [10] (p. 1). This is alarming because the transformation of plastic debris in the environment is not well understood yet. The persistence of these particles in natural ecosystems disrupts our environment’s ecological balance and impacts human health. Micro- and nanoplastic particles enter the human body via inhalation and absorption [1], permeate biological membranes [7], and bioaccumulate in organs. Nanoplastic particles have been found in human lungs, livers, spleens, kidneys, and the placentas of newborn babies [1,11–28]. Consequently, micro-

nanoplastic particle pollution is “. . . a potential threat to food security, health, and environment” [7] (p. 164533(1)) [29]. Moreover, plastic debris is hydrophobic and adsorbs pollutants on its surface at concentrations that are several orders of magnitude higher than in the surrounding water, acting as carriers of hazardous chemicals, which increases the pollutants’ bioavailability to aquatic and soil organisms [4,12,13,15,18].

Previous studies have demonstrated that conventional Wastewater Treatment Plants (WWTPs) are the main pathways for the release of micro- and nanoplastic particles. Currently, WWTPs normally remove, on average, a maximum of 90% of the micro- and nanoplastic particles contained in municipal and industrial wastewaters [4,5,7,10,19,24–26,30–32]. It has been reported that the average annual discharge of microplastic particles from 12 German WWTPs is around 2×10^9 microparticles, while the average discharge of microparticles (size range: 10–500 μm) from 10 large Danish WWTPs is 3 tonnes/year [8]. Furthermore, as stated by [4] (p. 2), “. . . around 50–85% of MPs [microplastics] could be retained in the sewage sludge, which is widely utilized as biofertilizer. . .” [4,31]. To give an example, it has been estimated that about 1.09×10^9 microparticles/day in the form of sludge enters the environment [8]. Hence, significant amounts of micro- and nanoplastic particles are globally discharged daily into the environment. Additionally, it has been identified that the shear forces [10] applied to plastic debris particles during customary water treatment processes cause the further fragmentation of larger plastic debris and microplastic particles into nano-size particulates, which aggravates the pollution problem [5,33].

WWTPs generally employ primary and secondary treatments. However, in some cases, the specifications, quality, and applications of the final treated water will determine if the application of tertiary treatment is required [34–36]. Tertiary treatments in WWTPs could include any of the following processes: filtration, ultrafiltration, precipitation, adsorption, reverse osmosis, evaporation, solvent extraction, crystallization, oxidation, electrolysis, and electrodialysis, among other processes [34,37,38]. According to [4] (p. 2), “. . . no specific treatment technology has been employed yet in WWTPs for the elimination of MPs and NPs [nanoplastics] from sewage excluding the treatment techniques . . . [that are] already available in WWTPs such as skimming, mesh screening, grit chamber, sedimentation, membrane bioreactor, and tertiary filtration” [4,26,31,38]. Early studies have demonstrated that tertiary processes commonly used in WWTPs remove, on average, up to 90% of MPPs [31]. For instance, an assessment conducted on 34 Sewage Treatment Plants (STPs) in New York indicated that conventional tertiary wastewater treatments, such as microfiltration and rapid sand filters, are partially effective in removing MPPs [8].

Therefore, there is renewed interest in researching and developing superior technologies to target the efficient removal of micro- and nanoplastic particles from water environments [4]. These advanced technologies include membrane technology (e.g., microfiltration and ultrafiltration) [10], bio-membrane composites [39], and nanotechnology [40]. These novel processes display different levels of performance and manufacturing costs [4,10,26,27,41–43]. Additionally, these advanced technologies are expensive and offer operational limitations, such as rapid fouling and membrane blockage [10,19,28,39,43–47]. Other technologies targeted to the removal of micro- and nanoplastic particles from wastewater “. . . are still at the laboratory-scale or preliminary research phase” [4] (p. 29) including air flotation [10], bioremediation, bio-nano filtration membranes, photodegradation, coagulation/flocculation, bio-based flocculants (e.g., chemically modified cellulose, lignin, chitin) electrooxidation, electrocoagulation, advanced oxidation processes, ultrasound, centrifugation [27], and magnetic separation [4,5,11,26,48–50].

The adsorption approach for the removal of micropollutants [51,52] from wastewater has the advantages of simplicity, high removal efficiency, and a wide range of applicability. Furthermore, the adsorption process is more cost-effective compared to other processes, such as membrane filtration and reverse osmosis, because these processes are more energy-intensive (e.g., high pressure requirements) and need routine costly maintenance procedures to control membrane fouling [43]. In the specific context of micro- and nanoparticle removal from wastewater, adsorption was shown to be highly effective [28,43,53], and it has

been considered one of the major approaches for removing microplastics [43]. Therefore, the development and evaluation of specially made adsorbents for the removal of nanoplastics and microplastics has attracted research interest. These include tailored activated carbons, carbon nanotubes, molecular sieves, sponges, aerogel, fibre materials, metal (hydr)oxides, zeolites, metal–organic frameworks (MOFs), covalent organic frameworks (COFs), and metal superhydrophobic magnetic adsorbents, among others [4,9,10,26,27,41,53,54]. The development of synthetic and bio-based adsorbents with superhydrophobic surfaces aims to increase the affinity among the adsorption sites of the adsorbent and micro- and nanoplastic particles [55]. Plastic materials display low charge densities (e.g., low surface energy) that render a hydrophobic surface due to the presence of long chains of C-H bonds [33,49]. Recent research has demonstrated that superhydrophobic materials are very effective in removing microplastic particles from water with efficiencies close to 100% [33].

The adsorption effectiveness of several carbon materials, including biochar [56], magnetic biochar, activated carbon, graphene oxide, magnetic carbon nanotubes [57], and Cu-Ni systems, among many others, toward micro- and nanoparticles from wastewater ranges from low (e.g., 25%) to high (e.g., 99%) [9,54,57]. Presently, activated carbon is the most used solid adsorbent in large-scale industries and in domestic water purification systems [58]. Although these carbon materials display wide-ranging adsorption capacities of MPPs, their main downside is high manufacturing costs because their production and activation processes are energy-intensive [9,35,37]. Thus, there is growing interest in the evaluation of eco-friendly and low-cost adsorbents, including natural materials, agricultural waste, and industrial by-products, which could be used with minimum pre-processing [9,51].

Bio-substrates are sustainable, renewable, economically viable, and safe [59–61], which is crucial in the context of large-scale applications. Furthermore, biomaterials are readily available, scalable, and currently used in the production of many industrial goods, including textile fabric, medical supplies, composites, twine, and ropes [62].

Recent studies have reported on the efficiency of native and/or modified bio-substrates as adsorbents for the removal of micro- and nanoparticles from drinking water and/or wastewaters, which include bio-nano adsorbents (e.g., lignin–zeolite composite nanofiber) [58], natural adsorbents such as zeolites and bentonites [63], biodegradable superhydrophobic sponges [64], and superhydrophobic cotton fabrics via chemical modification that display removal efficiencies of microplastic particles higher than 99% from water bodies [33]. Similarly, the surface modification of waste biomass, including coconut, sugarcane, and banana peel bagasse, has been evaluated using a non-ionic surfactant to increase the adsorption capacity toward microplastic particles from wastewater. This study demonstrated that the adsorption capacity ranged from 51% (e.g., treated coconut bagasse) to 80% (e.g., treated sugarcane bagasse) [65]. Native and chemically modified cellulose fibre-based adsorbents (e.g., cellulose nanofiber) show high efficiency in adsorbing MPPs from water [9,42,54]. Chitin-based sponges (e.g., chitosan nanofiber sponges) embedded with graphene oxide and oxygen-doped carbon nitride display removal efficiency of microplastics ranging from 72 to 92% [32,54]. The chemical modification of bio-substrates to make their surface superhydrophobic (e.g., low surface energy) for the efficient adsorption of microplastics from water [33] has been evaluated. The aim of this process is to support hydrophobic interactions between microplastics and the superhydrophobic adsorbents [54]. Protein-based materials (e.g., amyloid fibrils) demonstrated suitable adsorption of microplastics with removal rates up to 93% [54]. The adsorption mechanism of MPPs onto the amyloid fibrils is attributed to hydrophobic interactions with the protein side chains. Nevertheless, amyloid fibrils are very susceptible to the pH of the aqueous environment, which limits its applications [54].

Overall, the adsorption mechanisms involved in the removal of nano- and microplastic particles from water bodies depend on the type of adsorbent (e.g., specific surface area, morphology, surface charge, porosity, surface functional groups) [53], the composition of the aqueous media, pH, conductivity, temperature, the concentration, particle size, shape, and chemical structure of microplastics, etc. [49,53]. In general, adsorption mechanisms include

hydrophobic interactions, hydrogen-bond interactions, van der Waals forces, electrostatic interactions, π - π electron interaction, π - π electron conjugation, and complexations, among others [58,66].

Although the novel multifunctional adsorbent materials recently developed have demonstrated enhanced adsorption performance, some of these materials display potential health risks and adverse environmental impacts. Therefore, it is necessary to continue the research and development of new adsorbents that display higher adsorption capacities, selectivities, shorter adsorption times, ease of regeneration, low-cost, non-toxicity, biodegradable, and reusability [54] under the umbrella of the green chemistry principles.

In this exploratory research, cattail (*Typha Latifolia*) fibres were selected for evaluation as a bio-adsorbent because of the following key properties: natural hydrophobicity, biodegradability, non-toxicity, low-cost, and direct use without the need for pre-processing or chemical modifications. Therefore, we assumed that CFs could be suitable bio-adsorbents of microplastic residues from water bodies via hydrophobic interactions.

More specifically, this preliminary research design aimed to answer the following research questions. First, how effective are native hydrophobic CFs as bio-adsorbents of MPPs from wastewaters? and secondly, to what extent does the composition of the adsorption environment affect the adsorption rate of MPPs onto the CFs hydrophobic surface? To answer these research questions, straightforward batch adsorption tests were conducted using MPPs from the following polyolefins: polyvinyl chloride (PVC), polypropylene (PP), low-density polyethylene (LDPE), and high-density polyethylene (HDPE). According to [29] and [33], these polyolefins account for more than 60% of plastic waste. Furthermore, as stated by [5] (p. 6). "The most abundant NPs [nanoplastic particles] in sewage sludge are polyethylene (53%) and polypropylene (30%)". The polyamide, Nylon 6, was also used in this study. The effect of the composition of the adsorption environment on the adsorption process was evaluated using industrial wastewater and Type II Distilled Water.

The specific objectives of this exploratory research were as follows:

1. Characterization of the physicochemical properties of CFs.
2. Establishment of the efficiency of CFs as a hydrophobic bio-adsorbent of MPPs. Five MPP adsorbates of different plastic materials (e.g., PVC, PP, LDPE, HDPE, and Nylon 6) were evaluated.
3. Implementation of straightforward batch adsorption (e.g., static adsorption) tests to determine if physisorption of MPPs takes place on the hydrophobic surface of the CFs at ambient temperature. Batch adsorption tests were specifically implemented to differentiate if the removal of MPPs was due to spontaneous and instantaneous adsorption rather than mechanical retention of plastic debris (e.g., filtration).
4. Determination of the effect of the adsorption environment on the adsorption rate of MPPs onto the surface of CFs.
5. Establishment of the dominant mechanism driving the adsorption of microplastic MPPs onto the CFs' hydrophobic surface.

2. Experimental Methodology

2.1. Materials

2.1.1. Adsorbents: Cattail Fibres (CFs) and Activated Carbon (AC)

The CFs used in this work were locally sourced from several wild wetlands around the city of Fredericton, New Brunswick, Canada. The cattail fibres were sieved using a vibratory sieve shaker, model AS 200, manufactured by Retsch (Haan, North Rhine-Westphalia, Germany), at 60 rpm for an hour using a sieve No. 12 (opening 1.7 mm USA Standard Testing Sieve, ASTM-11 specification) to separate the seeds from the fibres.

The activated carbon (AC) used as a reference adsorbent was DARCO[®], Hydrodarco B, HDB, Batch 4-87, manufactured by American Norit Company, Inc. (Jacksonville, FL, USA).

2.1.2. Microplastic Particles (MPPs)

The MPP particles (randomly selected commercial polymers available in the laboratory) were subjected to particle size analysis to determine the weight average diameter. The procedure was carried out using a vibratory sieve shaker, model AS 200, manufactured by Retsch (Haan, North Rhine-Westphalia, Germany). Seven sieves, Canadian Standards Sieve Series (Ottawa, ON, Canada), were used in the following mesh No. order: 50, 60, 70, 100, 140, 200, and 325. Each of the MPPs particles was poured into the top sieve (i.e., mesh No. 50), and the sieve column was fixed using a lid equipped with adjusting screws and nuts at the top and a pan at the bottom. Then, the vibratory sieve shaker was run at 60 rpm for a period of 30 min. Afterward, the MPPs retained on each sieve were weighed and subsequently the weight average diameter was calculated for each microplastic particle material.

2.1.3. Adsorption Environment

Two adsorption environments were used: distilled water Type II and Produced Water (PW) from an Oil and Gas production operation. The produced water was provided by Cenovus Energy Inc. (Calgary, Alberta, Canada) from the Pelican Lake heavy oil operations in northern Alberta, Canada. The concentration of crude oil in the PW was 105 ppm, and the salinity concentration was 2.1 wt%.

2.2. Methodology

2.2.1. Cattail Fibre Characterization

CFs were characterized by employing several analytical techniques as follows. Fourier Transform Infrared Spectroscopy (FTIR) Analysis, which was carried out using a 6700 FTIR manufactured by Thermo Fisher Scientific (Waltham, Massachusetts, USA). The signals acquired were an average of 32 scans performed in the range of 400 cm^{-1} to 4000 cm^{-1} with a resolution of 4 and data spacing of 1.928 cm^{-1} . Background spectra were first collected with a KBr (~100 mg) pellet. An amount of 1 mg of cattail fibre was mixed with 99 mg of crushed KBr and then pressed into a pellet of 1 cm diameter. The spectra presented were background corrected. The thermogravimetric analysis (TGA) of the CFs was conducted using a TGA Q500 equipped with an EGA furnace (TA Instruments, New Castle, DE, USA). The Contact Angles of CFs and MPPs were obtained using a Goniometer, model G16-2, manufactured by Wet Scientific (Beaumont, TX, USA). The optical micrographs were obtained using an Olympus Compact Inverted Metallurgical Microscope, model GX41, manufactured by Olympus America Inc. (Breinigsville, PA, USA). The microscope was equipped with an Infinity2 Microscopy camera and the Infinity Analyze and Capture software (<https://www.lumenera.com/>, accessed on 27 February 2024), manufactured by Lumenera Corporation (Ottawa, ON, Canada) that were used to measure the diameter of the CFs. A scanning electron Model SU-70 (Hitachi, Tokyo, Japan) at an accelerating voltage of 5 kV was used to obtain high-resolution images of the CFs and detailed morphological information of the cattail fibres' surface. The surface area of the CFs and activated carbon was measured using a Quantachrome Autosorb 1-C manufactured by Quantachrome Instruments (Boynton Beach, FL, USA). The Brunauer–Emmett–Teller (BET) procedure was applied using nitrogen as the adsorbate gas.

2.2.2. Batch Adsorption Tests

Batch adsorption tests were conducted in such a way that the “spontaneous and instantaneous” adsorption of MPPs could take place on the surface of the hydrophobic cattail fibers without inducing the mechanical trapping of MPPs within the fibre network (e.g., filtration). The batch adsorption tests were carried out at ambient temperature (e.g., 24 °C) by placing a container with a flat bottom with the corresponding mass of microplastic particles. Then, 200 mL of distilled water (DW) or produced water (PW) was transferred onto the surface of the MPPs, which immediately floated to the surface of the liquid because the hydrophobicity of the plastic materials limits their dispersion in aqueous solutions [67,68]. Afterward, a fixed mass of cattail fibres (0.3 g) was placed on the surface

of the liquid, and the mixture was slightly stirred using a spatula for 30 s to aid further contact between the MPPs and the CFs. This stirring stage was carried out carefully to avoid the mechanical retention of the particles within the CFs network. Then, the mixture was left still for 10 min. After that, the cattail fibres and adsorbed MPPs were carefully extracted from the liquid surface with the help of tweezers onto a Petri dish. The Petri dish was placed in an oven at 45 °C for drying until the mass of the CF-MPP solid blend remained constant, which was indicative of total evaporation of the water initially contained in the CF-MPP system. Next, the weight of the CF-MPP solid mixture was determined to calculate the amount of microplastic particles adsorbed onto the surface of the CFs. Batch adsorption tests were repeated six times for each plastic material. Figure 1 displays the experimental set-up and the experimental procedure followed during the batch adsorption tests.

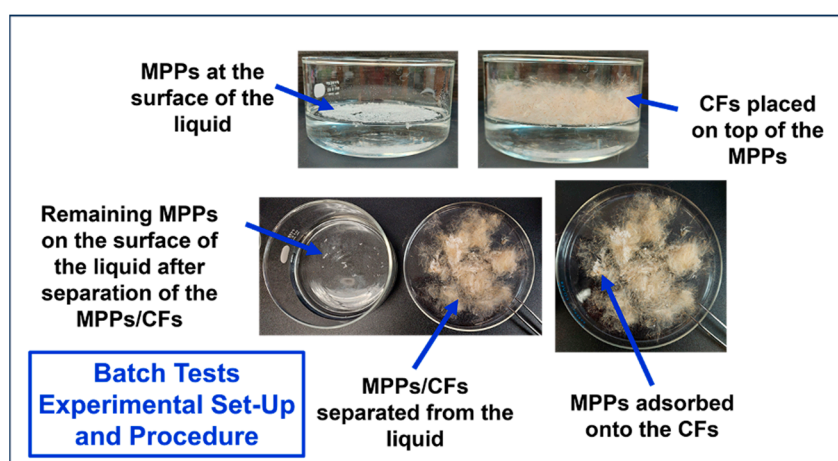


Figure 1. Batch adsorption tests: experimental set-up and procedure.

2.2.3. Experimental Design

Table 1 summarizes the experimental matrix indicating the type of plastic materials, the MPP solution concentrations, and the adsorption environments evaluated in this study. Fixed parameters, such as the mass of the adsorbent (e.g., CFs or AC) and the temperature of the adsorption process, are also indicated. Activated carbon was used as a baseline adsorbent material.

Table 1. Experimental Matrix.

Adsorbent Material	Microplastic Particles	Distilled Water, DW	Produced Water, PW
		Solution Concentration [wt%] Volume: 200 mL	Solution Concentration [wt%] Volume: 200 mL
CFs or AC 0.3 g T = 24 °C	PVC	0.1	0.1
		0.3	0.3
		0.5	0.5
	PP	0.1	0.1
		0.3	0.3
		0.5	0.5
	LDPE	0.1	0.1
		0.3	0.3
		0.5	0.5
	Nylon 6	0.1	0.1
		0.3	0.3
		0.5	0.5
	HDPE	0.1	0.1
		0.3	0.3
		0.5	0.5

2.2.4. Statistical Analysis

The experimental results were processed using Microsoft Excel software (Version 16.83) and expressed as the arithmetic mean \pm standard error of the mean. All graphs were plotted using Microsoft Excel.

3. Results and Discussion

3.1. Infrared Spectroscopy (FTIR) Analysis of Cattail Fibres

CFs are mainly composed of cellulose, hemicelluloses, and lignin [69]. Figure 2 displays the FTIR spectrum of CFs, which confirms the presence of typical functional groups associated with biomass materials. In Figure 2, the broadband between the wavenumbers of 3600 cm^{-1} to 3020 cm^{-1} is attributed to the hydroxy group, H-bonded OH stretch indicative of the presence of cellulose and hemicellulose [70–72]. The narrow peaks from 1650 cm^{-1} to 1550 cm^{-1} match alkenyl C=C and C-O stretching ascribed to lignin content [71–73]. Previous studies have demonstrated the presence of a waxy film on the CFs' surface, which makes these fibres hydrophobic [69,71,73–78]. The presence of a wax layer covering the fibres is confirmed by the narrow and weak peaks observed from 2920 cm^{-1} to 2850 cm^{-1} that correspond to the asymmetric and symmetric CH_2 and CH_3 stretching vibrations associated with aliphatic wax components [70,72,75]. The peak at 1740 cm^{-1} wavenumber corresponds to a carbonyl group (C=O) stretching vibration (e.g., carboxylic acid, aldehydes, ester, acetyl, etc.) in lignin and hemicellulose [70,72,73,79]. Other several narrow peaks from 1360 cm^{-1} to 1020 cm^{-1} represent several stretching vibrations related to -C-O, - CH_2 deformation, Si-C, C-O of cellulose, hemicelluloses, and lignin and C-N stretching [80].

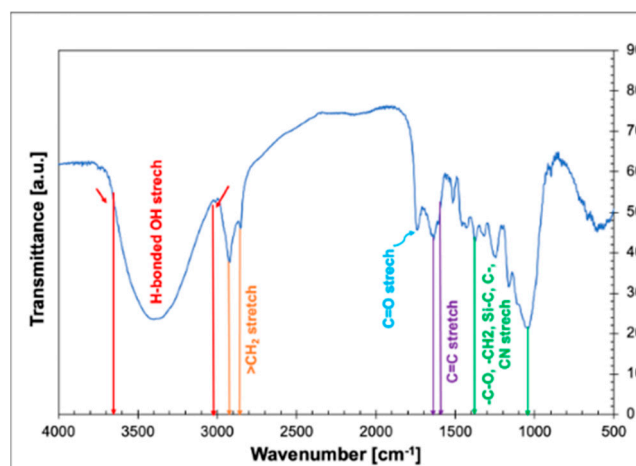


Figure 2. FTIR spectrum of cattail fibres.

3.2. Thermogravimetric Analysis (TGA) of Cattail Fibres

Figures 3a and 3b show the TGA and DGT thermograms of CFs, respectively. These thermograms show the initial dehydration of the CFs that started from $35\text{ }^{\circ}\text{C}$ to $124\text{ }^{\circ}\text{C}$. In this temperature range, approximately 6.2 wt% unbound and bound water was evaporated. The onset of thermal degradation reactions, which is determined from “the intersection of the initial baseline with the tangent of the plot at the steepest point” [81], started at $270\text{ }^{\circ}\text{C}$ with major degradation rates at $296\text{ }^{\circ}\text{C}$ and $336\text{ }^{\circ}\text{C}$ causing a weight loss of 46.1 wt%. These first thermal degradation reactions that finished at approximately $336\text{ }^{\circ}\text{C}$ are linked to the overlapping thermal decomposition of holocellulose, cellulose, hemicellulose, and lignin [82–84]. Earlier research has demonstrated that the thermal decomposition of lignin starts at approximately $290\text{ }^{\circ}\text{C}$ and continues slowly until about $440\text{ }^{\circ}\text{C}$ [83], a behaviour that is also observed in this study. This TGA analysis indicates that CFs are thermally stable up to $200\text{ }^{\circ}\text{C}$, which makes these fibres suitable for high-temperature applications.

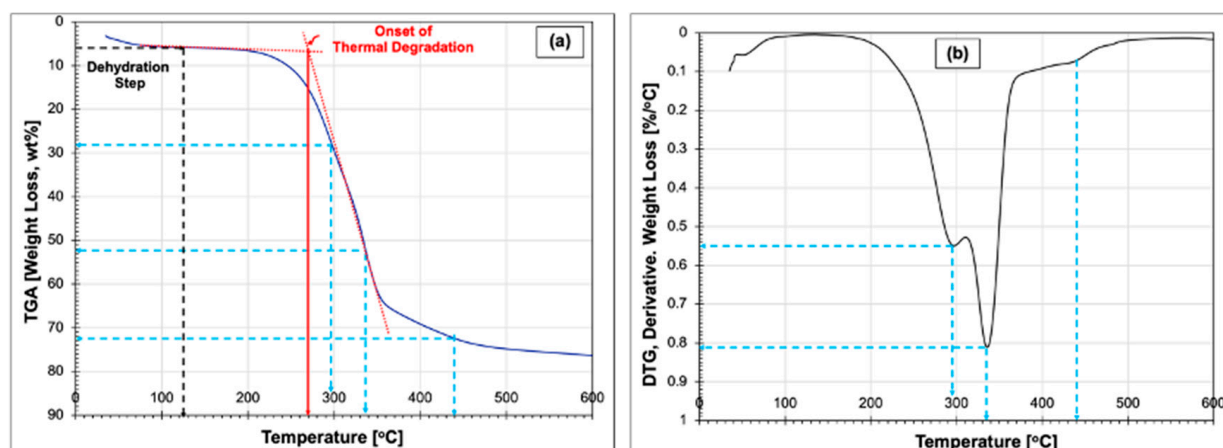


Figure 3. Thermogravimetric analysis: (a) TGA and (b) DTG thermograms.

3.3. Contact Angle of Cattail Fibres and MPPs

The measured contact angle, θ , of the CFs is $117^\circ \pm 2.83$ in distilled water. Therefore, the surface of native CFs is hydrophobic, as reported by several studies [69,73,75]. Previous research has demonstrated that the hydrophobicity of the CFs is explained by the high content of wax that forms a film on the fibre surface [85]. The reported wax content in CFs ranges from 6.13 wt% [76] to 11.5 wt% [77,85].

The measured contact angles (θ) in distilled water of the different MPP materials evaluated in this work are as follows: θ of Nylon 6 = $68.5^\circ \pm 5.5$, θ of PP = $111.1^\circ \pm 4.2$, θ of HDPE = $104.1^\circ \pm 1.9$, θ of LDPE = $102.5^\circ \pm 2.4$, and θ of PVC = $121^\circ \pm 0.9$. All the measured values of contact angle obtained in this work are within the same order of magnitude as the contact angle values reported in the literature [86–92] for these plastic materials. However, it is important to clarify that the contact angles were measured on the irregular shape of the microplastic particles that were carefully compacted on the Goniometer sample holder. The compacted MPP layers displayed rough, irregular surfaces. Therefore, the contact angle values reported in this work are toward the higher end of the range of the contact angle values reported in the literature. This observation is explained via the effect of surface roughness on contact angle measurements, which is explained "...by Wenzel, who stated that adding surface roughness will enhance the wettability caused by the chemistry of the surface. For example, if the surface is chemically hydrophobic, it will become even more hydrophobic when surface roughness is added" [93] (p. 1).

The measured contact angles of the MPP materials evaluated in this study further demonstrate the strong hydrophobic nature of PVC, PP, LDPE, and HDPE, while the contact angle of the MPPs of Nylon 6 at $\theta = 68.5^\circ \pm 5.5$ indicates its weak hydrophobicity compared with the other MPP materials tested here.

3.4. Optical and Scanning Electron Microscopy

Figure 4a displays a picture of CF fluff obtained after breaking the cattail flower. Figures 4b and 4c show an optical micrograph under visible light and under cross-polarized light, respectively. The optical microscope image under visible light displays a cluster of CFs with an average diameter of $22.8 \mu\text{m} (\pm 1.31)$ and a length of $9.55 \text{ mm} (\pm 0.302)$. The CF dimensions obtained in this study agree with the dimensions of CFs reported in the literature [75,84,94–96]. The micrograph (Figure 4c) obtained under cross-polarized light allows us to observe continuous films of bright white layers of waxy crystals on the surface of the fibres [97], which confirms the hydrophobic nature of CFs. The SEM micrograph—Figure 4d shows that CFs have a hollow structure with a rough surface. Morphology that in prior studies has been referred to as a "bamboo-shape structure" [75] (p. 28). The hollow structure of these fibres explains the high adsorption and retention capacity of CFs, as

previously reported [73,75]. The SEM micrograph also displays the waxy film (e.g., a bright white layer) covering the surface of the fibres [98].

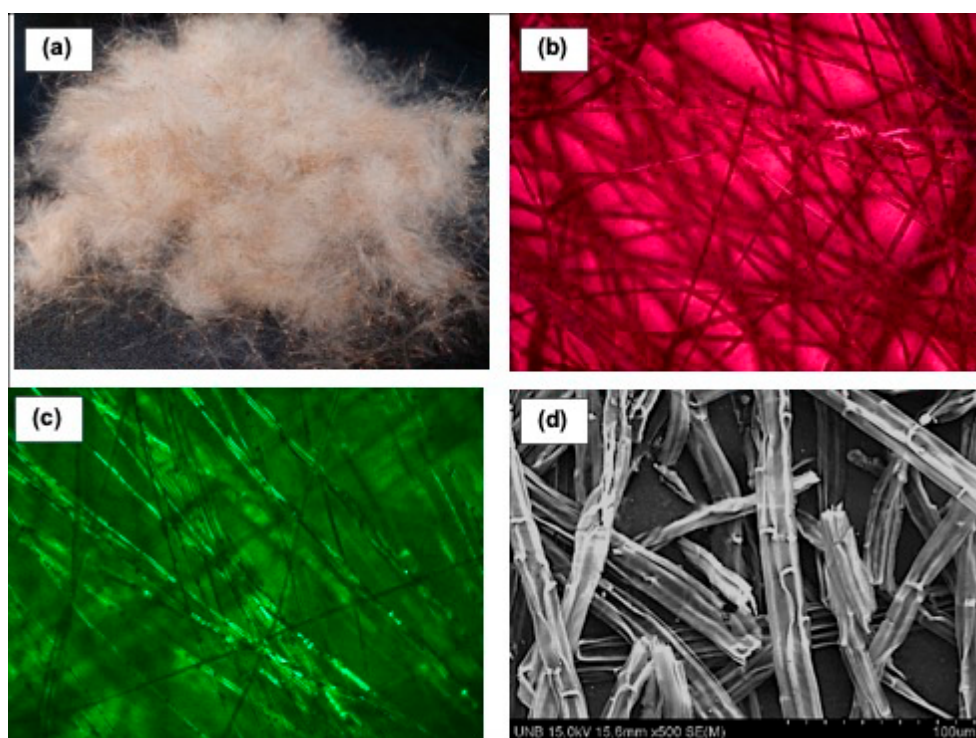


Figure 4. (a) Optical image of CFs fluff, (b) Optical microscope image (10×) of CFs under visible light, (c) optical microscope image (10×) of CFs under cross-polarized light and (d) SEM micrograph of CFs (500×).

3.5. Surface Area of CFs and Activated Carbon

The surface area of the CFs and the baseline commercial activated carbon was determined via BET analysis. The BET surface area of the CFs was $0.097 \text{ m}^2/\text{g}$ (± 0.037). This average value is within the detection limits of the equipment. Therefore, CFs could be considered as macroporous material with pore diameters greater than 50 nm [99]. The low surface area observed for CFs in this work agrees with the surface area reported for other bio-derived adsorbents, as is the case of Isabel grape bagasse [100]. The reference commercial activated carbon shows a surface area of $488 \text{ m}^2/\text{g}$, with a pore volume of $0.6921 \text{ cm}^3/\text{g}$ and an average pore diameter of 5.673 nm thus the baseline activated carbon falls within the “mesoporous” materials with pore widths ranging from 2 to 50 nm [99].

3.6. Sieve Analysis of Microplastic Particles

Figure 5a–e displays the histograms of the particle size distributions and the weight average diameters of each of the MPPs evaluated in this study. The inserted pictures within the histograms are optical micrographs displaying the morphology of the corresponding MPPs.

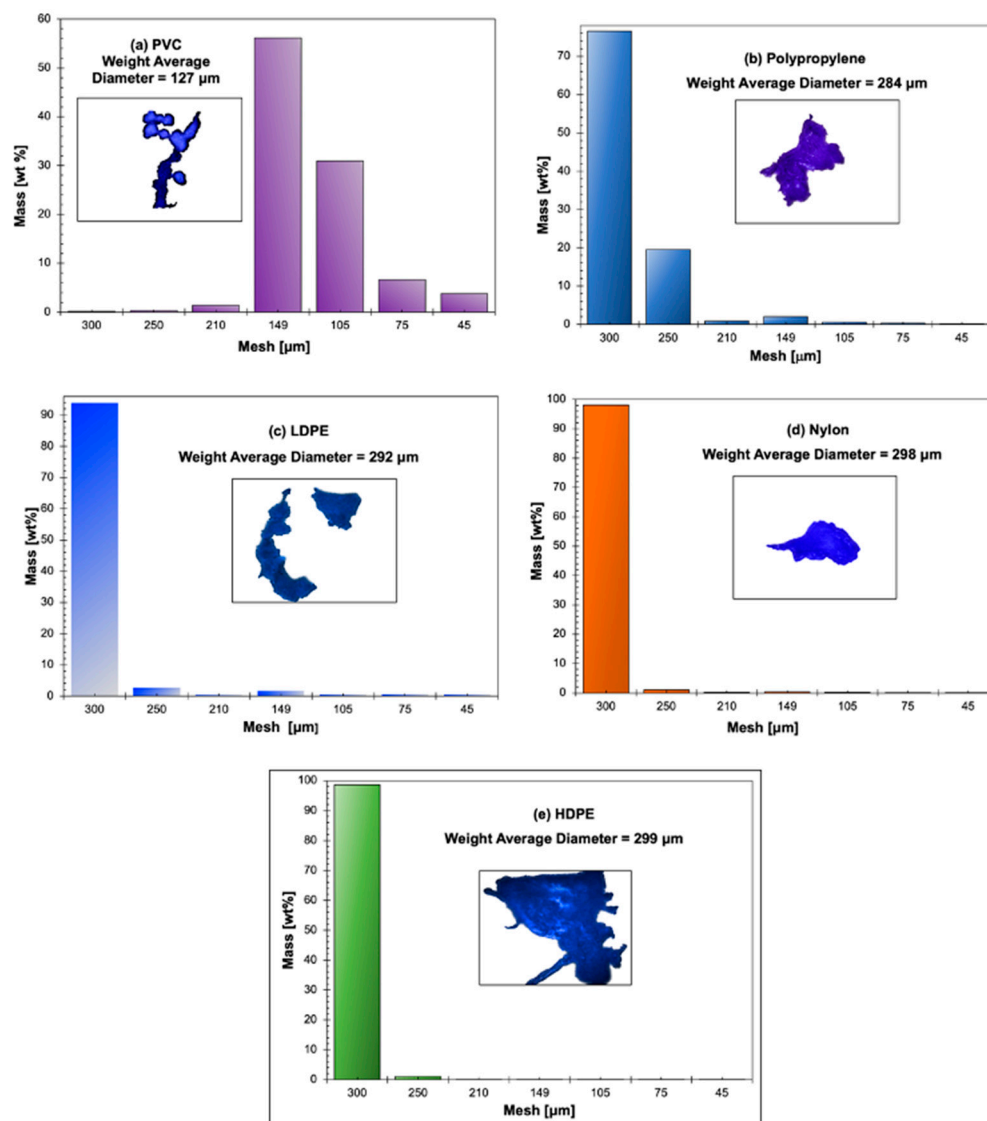


Figure 5. Histograms of the particle size distributions, weight average diameters, and optical micrographs of the plastics evaluated in this study. (a) poly(vinyl chloride) (PVC), (b) polypropylene (PP), (c) low-density polyethylene (LDPE), (d) Nylon 6, and (e) high-density polyethylene (HDPE).

Figure 5a–e shows that the PVC MPPs display the lowest weight average diameter at 127 μm , while the other MPP materials have weight average diameters ranging from 284 μm to 299 μm .

3.7. Batch Adsorption Tests of MMPs onto CFs

In this study, all the polyolefin MPPs show “spontaneous and instantaneous” adsorption onto the surface of the CFs, except for the polyamide Nylon 6. Figure 6a–j display the adsorption percentage of each of the MPPs onto the CFs as a function of the equilibrium concentration (e.g., c_e [mg/L]). The mass of CFs used during the batch adsorption tests was fixed at 0.3 gr, and three concentrations of MPPs in aqueous solutions: 0.1 wt%, 0.2 wt%, and 0.3 wt% were evaluated.

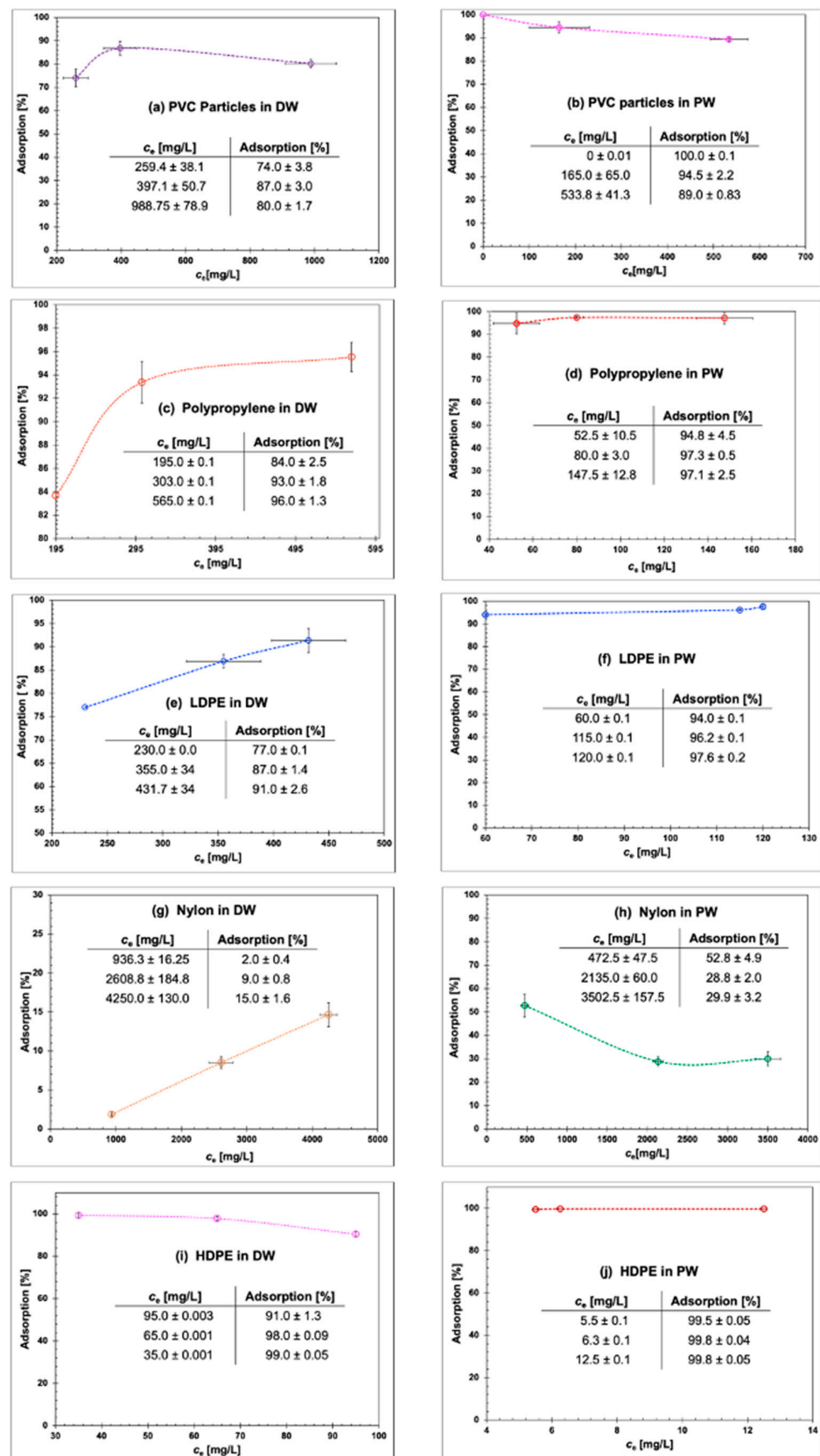


Figure 6. Adsorption [%] as a function of c_e [mg/L] for CFs. (a) PVC in DW, (b) PVC in PW, (c) PP in DW, (d) PP in PW, (e) LDPE in DW, (f) LDPE in PW, (g) Nylon 6 in DW, (h) Nylon 6 in PW, (i) HDPE in DW, and (j) HDPE in PW.

In DW as the adsorption environment, the adsorption of the MPPs tends to increase with the increase in MPP concentration. The adsorption of MPPs is also a function of the type of plastic material. The percentage of maximum adsorption of MPPs on the surface of CFs decreases in the following order: HDPE ($99\% \pm 0.05$) > PP ($96\% \pm 1.3$) > LDPE ($91\% \pm 2.6$) > PVC ($80\% \pm 1.7$) > Nylon 6 ($15\% \pm 1.6$). Overall, native hydrophobic CFs are highly efficient in adsorbing these MPP materials except for the Nylon 6 MPPs, which show the lowest adsorption percentage of $15\% \pm 1.6$. These experimental observations agree with the adsorption performance of nano- and microplastics achieved for chemically modified cellulose fibres [9,42,53,54].

Figure 7 displays the chemical structures of the plastic materials evaluated in this work. The non-polar nature of PVC, PP, LDPE, and HDPE is well-defined by the chemical structures of these plastics [101,102]. The chemical structure of Nylon 6 reveals its polarity via the amide group, which interacts with surfaces via hydrogen bonding [103]. Consequently, the low adsorption of Nylon 6 on the hydrophobic surface of the CFs is explained by the polarity of the Nylon 6 chemical structure (Figure 7d). Nylon contains numerous amine and acid functional groups [104,105], which decreases its affinity toward the hydrophobic surface of CFs. The adsorption behavior of Nylon 6 agrees with its measured contact angle at $\theta = 68.5^\circ \pm 5.5$ (Section 3.3), indicating that Nylon 6 is less hydrophobic than the other plastic materials evaluated in this work.

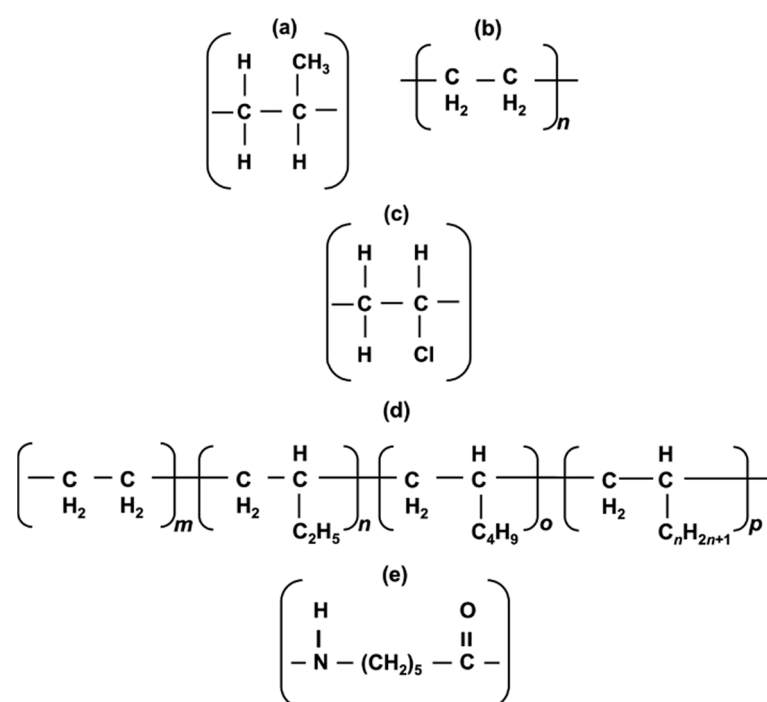


Figure 7. Chemical structures of the plastics used [adapted from [101]]. (a) Polypropylene (PP); (b) High-density polyethylene, (HDPE); (c) Polyvinyl chloride, (PVC) (d) Low-density polyethylene, (LDPE); (e) Polyamide (Nylon 6).

In PW as the adsorption environment, the presence of crude oil in the aqueous solution at a concentration of 105 ppm aids the adsorption of MPPs onto the CFs. Control tests were performed to evaluate the adsorption of the crude oil contained in the PW on the surface of the CFs. These control tests demonstrated that the crude oil is completely adsorbed onto the CFs. Therefore, prior to the quantification of the percentage of the MPPs adsorbed onto the CFs in PW, the amount of oil adsorbed onto the fibres was first subtracted. This allowed the independent quantification of the percentage of MPPs adsorbed onto the CFs. As previously indicated, the percentage of adsorption of all the MPPs significantly increased (e.g., >10% adsorption increase) in the presence of crude oil, which indicates that

the crude oil accelerates the adsorption of MPPs onto the surface of CFs (Figure 6b,d,f,h,j). For instance, the maximum % adsorption of Nylon 6 increased from $15\% \pm 1.6$ to 29.9 ± 3.2 (Figure 6g,h), which is almost a 50% of adsorption increase.

3.8. Adsorption Mechanism of MPPs onto the Hydrophobic CFs Surface

The batch adsorption experiments show that the adsorption process of non-polar MPPs onto the hydrophobic surface of CFs is spontaneous and instantaneous. Thus, the active adsorption sites on the natural fibre are rapidly occupied by the non-polar MPPs. Increasing the MPP concentration also increases the adsorption percentage to a limiting value that might be caused by steric hindrance among the absorbed MPPs. These experimental observations suggest the existence of strong hydrophobic interactions between the non-polar (e.g., HDPE, PP, LDPE, and PVC) plastic surfaces [29,67,68,102,106] and the hydrophobic “waxy” film on the CFs surface as verified via FTIR (Section 3.1). The experimental evidence obtained in this study suggests that hydrophobic interactions dominate the physisorption process of MPPs onto the hydrophobic surface of CFs. These experimental observation matches the research findings recently reported, in which synthetically produced hydrophobic and superhydrophobic adsorbents are very effective in adsorbing MPPs from water bodies via hydrophobic interactions as the dominant sorption mechanism. A few of these novel adsorbents include Poly(dimethylsiloxane) (PDMS)-coated nickel foams, adecyltrimethoxysilane (HTMS)-nano-Fe [54], biomass-derived superhydrophobic sponges [64], surfactant-modified biomass bagasse [65], carbon nanotubes (CNTs) [57], modified superhydrophobic magnetic Fe₃O₄ nanoparticles [55], superhydrophobic cotton fabrics [33], and amyloid fibres (e.g., protein-based adsorbents) [54].

As clearly explained by [107] (p. 2711), “...the attractive force results from the increased dynamic structuring of water in the vicinity of nonpolar species incapable of hydrogen bonding with water...[that]...leads to a large interfacial energy and a consequent thermodynamic driving force to reduce the total amount of structured water. This is accomplished by bringing the nonpolar surfaces into contact, thereby eliminating water-nonpolar interfaces” [107]. Consequently, the strong interaction between the non-polar MPPs and the hydrophobic surface of CFs is driven by nonelectrostatic interactions [108]. This hydrophobic effect is the result of “...a strong attractive force between nonpolar species interacting across an aqueous medium...[that] is related to the low solubility of nonpolar species in water...” [107] (pp. 2722–2712).

This hydrophobic effect was experimentally demonstrated in our study by the fact that the adsorption of Nylon 6, which is intrinsically polar [109], onto the waxy surface of CFs was substantially negligible compared to the adsorption behaviour of the other non-polar MPPs. As Figure 6g shows, the maximum % adsorption of Nylon 6 onto the CF surface was $15\% \pm 1.6$ (Figure 6g) in distilled water as the adsorption environment. The driving force for the interaction of this polyamide with the CFs might be via hydrogen bonding among the polymer amide groups and the oxygen-containing functional groups (e.g., hydroxy and/or carboxylic acid) on the CFs surface [110] as indicated by the FTIR analysis (Section 3.1). However, the occurrence of these interactions seems minimum, as demonstrated by the insignificant adsorption behavior of Nylon 6 MPPs onto CFs.

The adsorption behavior of the MPPs was evidently affected by the composition of the aqueous media. Industrial-produced water (PW) from oil and gas recovery operations contains free and dispersed crude oil, dissolved organic compounds, salts, sulphates, nitrates, and suspended sand particles [111], among others. It is well established that “...the surrounding chemical environment affects hydrophobic interactions. [Therefore,] the presence of various additives in solution [for example] dissolved salt ions affect the solubility and interactions of hydrophobic species in water” [112] (p. 278). Consequently, it is possible to regulate the adsorption process by changing the composition of the aqueous media and/or “binding environment” [108]. Furthermore, the addition of lyophobic components to the “binding environment enhances the adsorption rates onto hydrophobic

surfaces "... at the level of both fluid-phase [adsorbate] transport and [adsorbate] binding to the surface" [107] (p. 2718).

In this work, the crude oil contained in the PW acts as a lyophobic component that markedly enhances the adsorption rates of the MPPs onto the waxy surface of the CFs (Figure 6a–j). Our experimental results concur with a similar study that evaluated the removal efficiency of MPPs by a superhydrophobic cotton adsorbent, in which the adsorption efficiency significantly increased when drops of hexane were added to the aqueous solution [33]. These researchers concluded that the presence of oil promotes the migration of MPPs toward the superhydrophobic adsorbent, and hydrophobic interactions dominate over electrostatic interactions. In this modified environment (e.g., the presence of oil), the binding energy of microplastics increases, and the Hamaker constant becomes positive [33].

Therefore, in the present study, the crude oil in the PW "... changes the state of hydration of the surface and the [MPPs]. The dehydration of hydrophobic areas resulting from binding and the entropy gain associated with it, lower the Gibbs energy of the system, driving the adsorption process" [108] (pp. 6356–6359).

Figure 8 displays micrographs of PVC (adsorption environment: distilled water) and HDPE (adsorption environment: PW) MPPs adsorbed onto the surface of CFs. These images clearly show the firm "attachment" of the MPPs to the CFs. In the case of PVC, in which the adsorption media was distilled water, the PVC microparticles appear as cotton balls adsorbed onto CFs. In contrast, the adsorption media for HDPE in this picture was PW; thus, the originally white HDPE microparticles appear darker in this image, which indicates that the microplastic particles were covered by a very thin layer of crude oil.

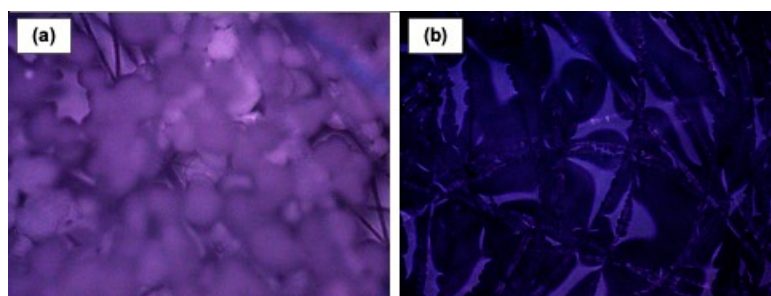


Figure 8. (a) PVC MPPs adsorbed onto CFs in DW as the adsorption environment; (b) HDPE MPPs adsorbed onto CFs in PW as the adsorption environment.

A commercial activated carbon (AC) was used in this study as a reference adsorbent to evaluate its efficiency in removing microplastic particles from aqueous media. The experimental observations indicated that this specific AC was inefficient in removing MPPs. Previous research has provided mixed observations in terms of the effectiveness of carbon materials in adsorbing nano- and microparticles. Overall, carbon-based adsorbent materials specifically applied for the removal of MPPs from aqueous media display wide-ranging adsorption efficiency of MPPs, with removal efficiencies ranging from low (e.g., up to 25% removal) [9,26], medium (e.g., 50 to 75%) [9], to high (e.g., >99%) as is in the case of magnetic carbon nanotubes type adsorbents and some granular activated carbons [43]. Recent studies have demonstrated that to increase the adsorption capacity of carbon materials toward MPPs, it is necessary to modify the porous morphology and the active vacant sites and to functionalize the adsorbent surface by incorporating different metals, metal oxides, and strong oxidizing agents to enhance the sorption ability [53,54].

On the contrary, our experimental results indicate that activated carbon particles were adsorbed onto the microplastic particle surface. These experimental observations indirectly demonstrate the capacity of MPPs to function as carriers and/or vectors for the transport of pollutant compounds in water bodies (e.g., toxic organic components), as has been reported in the literature [112,113]. Figure 9 displays a micrograph that shows activated carbon adsorbed onto the surface of polypropylene (PP) MPPs.

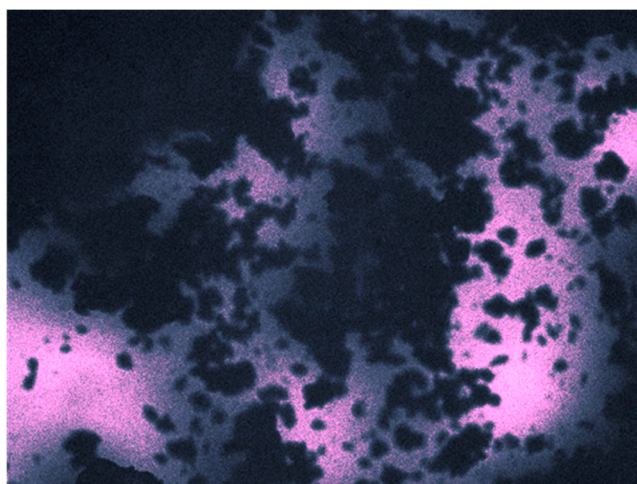


Figure 9. Micrograph of activated carbon adsorbed onto the surface of PP MPPs.

4. Conclusions

This straightforward exploratory research design demonstrates the effective adsorption of several MPP materials onto the hydrophobic surface of CFs. The experimental outcome supports our hypothesis. In distilled water, as the adsorption environment, the adsorption of MPPs ranged from 74% to 99% for PVC, PP, LDPE, and HDPE. In distilled water, the maximum adsorption of Nylon 6 was 15%. The low adsorption of Nylon 6 on the CFs' surface is attributed to its polarity, which prevents its adsorption onto the hydrophobic surface of the CFs. However, it was established that modifying the adsorption environment by adding lyophobic components (e.g., crude oil contained in the produced water, PW) to the adsorption media significantly enhances the rate of adsorption of MPPs onto the hydrophobic surface of the CFs. In PW, the adsorption percentage ranged from 89% to 100% for PVC, PP, LDPE, and HDPE. The adsorption of Nylon 6 increased to 29.9%, which corresponds to an adsorption enhancement of 50%. These experimental observations indicate that hydrophobic interactions are the dominant mechanisms driving the "spontaneous and instantaneous" adsorption of MPPs onto the CFs. It was also confirmed that it is possible to modify the adsorption environment by adding lyophobic components to effectively increase the adsorption rate of MPPs onto the hydrophobic surface of the CFs without increasing the mass of bio-adsorbent required. Indirectly, this exploratory study also demonstrated the capacity of MPPs to function as carriers and/or vectors of other compounds (e.g., pollutants) in water bodies.

Native hydrophobic cattail fibres show to be efficient, non-toxic, biodegradable, environmentally friendly, sustainable, low-cost, and reliable bio-adsorbents. The outcome of this research demonstrates the important role that natural hydrophobic bio-substrates could play in the reduction and control of the environmental nano- and microplastic particle pollution caused by the globalized human mismanagement of post-consumer plastics.

Nevertheless, more research is justified since this preliminary exploratory research design was intended to gain insights into the "spontaneous and instantaneous" physisorption of MPPs onto the hydrophobic surface of the CFs using straightforward batch adsorption tests. The most important fact is that the knowledge obtained from this exploratory research design allowed us to establish a more systematic investigation to establish in detail the effectiveness of hydrophobic CFs in adsorbing MPPs in more practical situations. Therefore, the undergoing phase of this investigation consists of the meticulous determination of the adsorption isotherms and the overall dynamics and adsorption kinetics via fixed-bed adsorption columns. The aim is to gather experimental information on the breakthrough concentration profiles to scale up our process for practical applications. Furthermore, the regeneration of the CFs will be studied and evaluated to determine the optimum regeneration conditions.

Author Contributions: Conceptualization, L.R.-Z. and D.R.; Data curation, L.R.-Z. and K.P.B.; Formal analysis, L.R.-Z. and K.P.B.; Funding acquisition, L.R.-Z.; Investigation, K.P.B. and L.R.-Z.; Methodology, L.R.-Z.; Resources, D.R. and L.R.-Z.; Supervision, L.R.-Z.; Validation, L.R.-Z. and D.R.; Writing—original draft, L.R.-Z.; Writing—review & editing, L.R. and D.R. All authors have read and agreed to the published version of the manuscript.

Funding: This research received no external funding.

Data Availability Statement: Data are contained within the article.

Acknowledgments: The authors wish to acknowledge Kyle Rogers, Chemical Engineering Department, University of New Brunswick, for his contributions in obtaining the FTIR spectrum and the TGA analysis of the cattail fibres. The financial support of the University of New Brunswick via the University Research Fund is also recognized.

Conflicts of Interest: The authors declare no conflict of interest.

References

1. Our Planet is Choking on Plastic. UN Environment Programme. Available online: https://www.unep.org/interactives/beat-plastic-pollution/?gad_source=1&gclid=EAIaIQobChMI-Yf4r5ehhAMVf2IHAR0ldQeREAAAYASAAEgIN3_D_BwE (accessed on 10 February 2024).
2. Kang, H.; Washington, A.; Capobianco, M.D.; Yan, X.; Cruz, V.V.; Weed, M.; Johnson, J.; Johns, G., III; Brudvig, G.W.; Pan, X.; et al. Concentration-Dependent Photocatalytic Upcycling of Poly (ethylene terephthalate) Plastic Waste. *ACS Mater. Lett.* **2023**, *5*, 3032–3041. [[CrossRef](#)] [[PubMed](#)]
3. Li, C.; Kong, X.Y.; Lyu, M.; Tay, X.T.; Đokić, M.; Chin, K.F.; Yang, C.T.; Lee, E.K.; Zhang, J.; Tham, C.Y.; et al. Upcycling of non-biodegradable plastics by base metal photocatalysis. *Chem* **2023**, *9*, 2683–2700. [[CrossRef](#)]
4. Ali, I.; Ding, T.; Peng, C.; Naz, I.; Sun, H.; Li, J.; Liu, J. Micro-and nanoplastics in wastewater treatment plants: Occurrence, removal, fate, impacts and remediation technologies—A critical review. *Chem. Eng. J.* **2021**, *423*, 130205. [[CrossRef](#)]
5. Mohana, A.A.; Farhad, S.M.; Haque, N.; Pramanik, B.K. Understanding the fate of nano-plastics in wastewater treatment plants and their removal using membrane processes. *Chemosphere* **2021**, *284*, 31430. [[CrossRef](#)] [[PubMed](#)]
6. Cao, R.; Xiao, D.; Wang, M.; Gao, Y.; Ma, D. Solar-driven photocatalysis for recycling and upcycling plastics. *Appl. Catal. B Environ.* **2024**, *341*, 123357. [[CrossRef](#)]
7. Briassoulis, D. Agricultural plastics as a potential threat to food security, health, and environment through soil pollution by microplastics: Problem definition. *Sci. Total Environ.* **2023**, *892*, 164533. [[CrossRef](#)] [[PubMed](#)]
8. Lakshmi, B.Y.; Sundaram, B.; Muthukumar, S. Microplastics in Wastewater. A Review of the Current Knowledge on Detection, Occurrence, and Removal. In *Emerging Technologies in Wastewater Treatment*, 1st ed.; Shah, M.P., Ed.; Taylor & Francis Group: Boca Raton, FL, USA, 2023; pp. 199–212.
9. Chen, Z.; Fang, J.; Wei, W.; Ngo, H.H.; Guo, W.; Ni, B.J. Emerging adsorbents for micro/nanoplastics removal from contaminated water: Advances and perspectives. *J. Clean. Prod.* **2022**, *371*, 133676. [[CrossRef](#)]
10. Pramanik, B.K.; Pramanik, S.K.; Monira, S. Understanding the fragmentation of microplastics into nano-plastics and removal of nano/microplastics from wastewater using membrane, air flotation and nano-ferrofluid processes. *Chemosphere* **2021**, *282*, 131053. [[CrossRef](#)]
11. Chen, Z.; Liu, X.; Wei, W.; Chen, H.; Ni, B.J. Removal of microplastics and nanoplastics from urban waters: Separation and degradation. *Water Res.* **2022**, *221*, 118820. [[CrossRef](#)]
12. Anderson, J.C.; Park, B.J.; Palace, V.P. Microplastics. *Environ. Pollut.* **2016**, *218*, 269–280. [[CrossRef](#)]
13. Zhou, Y.; Liu, X.; Wang, J. Ecotoxicological effects of microplastics. *J. Hazard. Mater.* **2020**, *392*, 122273. [[CrossRef](#)] [[PubMed](#)]
14. Chen, Y.; Liu, X.; Leng, Y.; Wang, J. Defense responses in earthworms (*Eisenia fetida*) exposed to low-density polyethylene microplastics in soils. *Ecotoxicol. Environ. Saf.* **2020**, *187*, 109788. [[CrossRef](#)] [[PubMed](#)]
15. Jiang, X.; Chang, Y.; Zhang, T.; Qiao, Y.; Klobučar, G.; Li, M. Toxicological effects of polystyrene microplastics on earthworm (*Eisenia fetida*). *Environ. Pollut.* **2020**, *259*, 113896. [[CrossRef](#)] [[PubMed](#)]
16. Woods, M.N.; Hong, T.J.; Baughman, D.; Andrews, G.; Fields, D.M.; Matrai, P.A. Accumulation and effects of microplastic fibers in American lobster larvae (*Homarus americanus*). *Mar. Pollut. Bull.* **2020**, *157*, 111280. [[CrossRef](#)] [[PubMed](#)]
17. Sierra, I.; Chialanza, M.R.; Faccio, R.; Carrizo, D.; Fornaro, L.; Pérez-Parada, A. Identification of microplastics in wastewater samples by means of polarized light optical microscopy. *Environ. Sci. Pollut. Res.* **2020**, *27*, 7409–7419. [[CrossRef](#)] [[PubMed](#)]
18. Rodríguez-Seijo, A.; Santos, B.; Ferreira da Silva, E.; Cachada, A.; Pereira, R. Low-density polyethylene microplastics as a source and carriers of agrochemicals to soil and earthworms. *Environ. Chem.* **2018**, *16*, 8–17. [[CrossRef](#)]
19. De Falco, F.; Di Pace, E.; Cocca, M.; Avella, M. The contribution of washing processes of synthetic clothes to microplastic pollution. *Sci. Rep.* **2019**, *9*, 6633. [[CrossRef](#)] [[PubMed](#)]
20. Wang, J.; Coffin, S.; Sun, C.; Schlenk, D.; Gan, J. Negligible effects of microplastics on animal fitness and HOC bioaccumulation in earthworm *Eisenia fetida* in soil. *Environ. Pollut.* **2019**, *249*, 776–784. [[CrossRef](#)] [[PubMed](#)]

21. Maes, T.; Jessop, R.; Wellner, N.; Haupt, K.; Mayes, A.G. A rapid-screening approach to detect and quantify microplastics. *Sci. Rep.* **2017**, *7*, 44501. [[CrossRef](#)]
22. Huntington, A.; Corcoran, P.L.; Jantunen, L.; Thaysen, C.; Bernstein, S.; Stern, G.A.; Rochman, C.M. A first assessment of microplastics and other anthropogenic particles in Hudson Bay and the surrounding eastern Canadian Arctic waters of Nunavut. *Facets* **2020**, *5*, 432–454. [[CrossRef](#)]
23. Mintenig, S.M. Low numbers of microplastics detected in drinking water from ground water sources. *Sci. Total Environ.* **2019**, *648*, 631–635. [[CrossRef](#)] [[PubMed](#)]
24. Sutton, R.; Mason, S.A.; Stanek, S.K.; Willis-Norton, E.; Wren, I.F.; Box, C. Microplastic contamination in the san francisco bay, California, USA. *Mar. Pollut. Bull.* **2016**, *109*, 230–235. [[CrossRef](#)] [[PubMed](#)]
25. Magnusson, K.; Norén, F. *Screening of Microplastic Particles*; Swedish Environmental Research Institute: Stockholm, Sweden, 2014.
26. Rout, P.R.; Mohanty, A.; Sharma, A.; Miglani, M.; Liu, D.; Varjani, S. Micro-and nanoplastics removal mechanisms in wastewater treatment plants: A review. *J. Hazard. Mater. Adv.* **2022**, *6*, 100070. [[CrossRef](#)]
27. Murray, A.; Örmeci, B. Removal effectiveness of nanoplastics (<400 nm) with separation processes used for water and wastewater treatment. *Water* **2020**, *12*, 635. [[CrossRef](#)]
28. Gao, W.; Zhang, Y.; Mo, A.; Jiang, J.; Liang, Y.; Cao, X.; He, D. Removal of microplastics in water: Technology progress and green strategies. *GAC Green Anal. Chem.* **2022**, *3*, 100042. [[CrossRef](#)]
29. Jiang, Y.; Zhang, H.; Hong, L.; Shao, J.; Zhang, B.; Yu, J.; Chu, S. An integrated plasma-photocatalytic system for upcycling of polyolefin plastic. *ChemSusChem* **2023**, *28*, e202300106. [[CrossRef](#)] [[PubMed](#)]
30. Ziajahromi, S.; Neale, P.A.; Rintoul, L.; Leusch, F.D. Wastewater treatment plants as a pathway for microplastics: Development of a new approach to sample wastewater-based microplastics. *Water Res.* **2017**, *112*, 93–99. [[CrossRef](#)] [[PubMed](#)]
31. Iyare, P.U.; Ouki, S.K.; Bond, T. Microplastics removal in wastewater treatment plants: A critical review. *Environ. Sci. Water Res. Technol.* **2020**, *6*, 2664–2675. [[CrossRef](#)]
32. Sun, C.; Wang, Z.; Zheng, H.; Chen, L.; Li, F. Biodegradable and re-usable sponge materials made from chitin for efficient removal of microplastics. *J. Hazard. Mater.* **2021**, *420*, 126599. [[CrossRef](#)]
33. Rius-Ayra, O.; Carmona-Ruiz, M.; Llorca-Isern, N. Superhydrophobic cotton fabrics for effective removal of high-density polyethylene and polypropylene microplastics: Insights from surface and colloidal analysis. *J. Colloid Interface Sci.* **2023**, *646*, 763–774. [[CrossRef](#)]
34. Hendricks, D. *Fundamentals of Water Treatment Unit Processes: Physical, Chemical, and Biological*; CRC Press: Boca Raton, FL, USA, 2016; pp. 3–19.
35. Shah, M.P. (Ed.) *Emerging Technologies in Wastewater Treatment*; Taylor & Francis Group: Boca Raton, FL, USA, 2023; pp. 1–249.
36. Islam, S.U. (Ed.) *Environmental Nanotechnology for Water Purification*; John Wiley & Sons: Hoboken, NJ, USA, 2020; pp. 1–329.
37. Deepti, P.M.; Purkait, M.K. Emerging Technologies and Their Advancements Toward Wastewater Treatment from Various Industries. In *Emerging Technologies in Wastewater Treatment*; Shah, M., Ed.; Taylor & Francis Group: Boca Raton, FL, USA, 2023; pp. 51–66.
38. Zhang, Y.; Jiang, H.; Bian, H.; Wang, H.; Wang, C. A critical review of control and removal strategies for microplastics from aquatic environments. *J. Environ. Chem. Eng.* **2021**, *9*, 105463. [[CrossRef](#)]
39. Yogarathinam, L.T.; Usman, J.; Othman, M.H.; Ismail, A.F.; Goh, P.S.; Gangasalam, A.; Adam, M.R. Low-cost silica based ceramic supported thin film composite hollow fiber membrane from guinea corn husk ash for efficient removal of microplastic from aqueous solution. *J. Hazard. Mater.* **2022**, *424*, 127298. [[CrossRef](#)] [[PubMed](#)]
40. Agarwal, P.; Prakash, S.; Saini, G. Natural Coagulants (*Moringa oleifera* and *Benincasa hispida*) based removal of Microplastics. *Clean. Water.* **2024**, *1*, 100010. [[CrossRef](#)]
41. Liu, Y.; Sun, J.; Yuan, J.; Wang, S.; Ding, Y.; Wu, Y.; Gao, C. A type of thiophene-bridged silica aerogel with a high adsorption capacity. *Inorg. Chem. Front.* **2018**, *5*, 1894–1901. [[CrossRef](#)]
42. Batool, A.; Valiyaveetil, S. Surface functionalized cellulose fibers—a renewable adsorbent for removal of plastic nanoparticles from water. *J. Hazard. Mater.* **2021**, *413*, 125301. [[CrossRef](#)] [[PubMed](#)]
43. Ahmed, R.; Hamid, A.K.; Krebsbach, S.A.; He, J.; Wang, D. Critical review of microplastics removal from the environment. *Chemosphere* **2022**, *293*, 133557. [[CrossRef](#)] [[PubMed](#)]
44. Snyder, S.A.; Westerhoff, P.; Yoon, Y.; Sedlak, D.L. Pharmaceuticals, personal care products, and endocrine disruptors in water: Implications for the water industry. *Environ. Eng. Sci.* **2003**, *20*, 449–469. [[CrossRef](#)]
45. Kasprzyk-Hordern, B.; Dinsdale, R.M.; Guwy, A.J. The occurrence of pharmaceuticals, personal care products, endocrine disruptors and illicit drugs in surface water in South Wales, UK. *Water Res.* **2008**, *42*, 3498–3518. [[CrossRef](#)] [[PubMed](#)]
46. Nilsen, E.; Smalling, K.L.; Ahrens, L.; Gros, M.; Miglioranza, K.S.; Picó, Y.; Schoenfuss, H.L. Critical review: Grand challenges in assessing the adverse effects of contaminants of emerging concern on aquatic food webs. *Environ. Toxicol. Chem.* **2019**, *38*, 46–60. [[CrossRef](#)]
47. Kim, S.D.; Cho, J.; Kim, I.S.; Vanderford, B.J.; Snyder, S.A. Occurrence and removal of pharmaceuticals and endocrine disruptors in South Korean surface, drinking, and waste waters. *Water Res.* **2007**, *41*, 1013–1021. [[CrossRef](#)]
48. Chowdhury, S.R.; Razzak, S.A.; Hassan, I.; Hossain, M.M. Microplastics in Freshwater and Drinking Water: Sources, Impacts, Detection, and Removal Strategies. *Water Air Soil Pollut.* **2023**, *234*, 673. [[CrossRef](#)]

49. Magalhães, S.; Alves, L.; Medronho, B.; Romano, A.; Rasteiro, M.D. Microplastics in ecosystems: From current trends to bio-based removal strategies. *Molecules* **2020**, *25*, 3954. [[CrossRef](#)] [[PubMed](#)]
50. Liu, X.; Li, M.C.; Lu, Y.; Li, Z.; Liu, C.; Liu, Z.; Mei, C.; Wu, Q. Cellulose nanofiber-coated delignified wood as an efficient filter for microplastic removal. *Prog. Nat. Sci. Mater. Int.* **2024**, in press.
51. Islam, M.R.; Rahman, M.S. *Sustainable Water Purification*; John Wiley & Sons: Hoboken, NJ, USA, 2020; p. 329.
52. Quintelas, C.; Mesquita, D.; Campos Ferreira, E. Bio Strategies for the Removal of Contaminants of Emerging Concern from Wastewater. In *Emerging Technologies in Waste Water Treatment*; Shah, M., Ed.; CRC Press: Boca Raton, FL, USA, 2023; pp. 171–183.
53. Ali, I.; Tan, X.; Li, J.; Peng, C.; Wan, P.; Naz, I.; Duan, Z.; Ruan, Y. Innovations in the development of promising adsorbents for the remediation of Microplastics and Nanoplastics—A critical review. *Water Res.* **2023**, *230*, 119526. [[CrossRef](#)] [[PubMed](#)]
54. Liu, Q.; Khor, S.M. Emerging absorption-based techniques for removing microplastics and nanoplastics from actual water bodies. *TrAC Trends Anal. Chem.* **2024**, *170*, 117465. [[CrossRef](#)]
55. Wang, H.P.; Huang, X.H.; Chen, J.N.; Dong, M.; Nie, C.Z.; Qin, L. Modified superhydrophobic magnetic Fe₃O₄ nanoparticles for removal of microplastics in liquid foods. *Chem. Eng. J.* **2023**, *476*, 146562. [[CrossRef](#)]
56. Siipola, V.; Pflugmacher, S.; Romar, H.; Wendling, L.; Koukari, P. Low-Cost Biochar Adsorbents for Water Purification Including Microplastics Removal. *Appl. Sci.* **2020**, *10*, 788. [[CrossRef](#)]
57. Tang, Y.; Zhang, S.; Su, Y.; Wu, D.; Zhao, Y.; Xie, B. Removal of microplastics from aqueous solutions by magnetic carbon nanotubes. *Chem. Eng. J.* **2021**, *406*, 126804. [[CrossRef](#)]
58. Chellasamy, G.; Kiriyanthan, R.M.; Maharajan, T.; Radha, A.; Yun, K. Remediation of microplastics using bionanomaterials: A review. *Environ. Res.* **2022**, *208*, 112724. [[CrossRef](#)] [[PubMed](#)]
59. Ansari, S.A.; Khan, F.; Ahmad, A. Cauliflower leave, an agricultural waste biomass adsorbent, and its application for the removal of MB dye. *Int. J. Anal. Chem.* **2016**, *252*–261.
60. Bedia, J.; Peñas-Garzón, M.; Gómez-Avilés, A.; Rodríguez, J.J.; Belver, C. A review on the synthesis and characterization of biomass-derived carbons. *C* **2018**, *4*, 63. [[CrossRef](#)]
61. Reddy, N.; Yang, Y. Properties and potential applications of natural cellulose fibers from cornhusks. *Green Chem.* **2005**, *7*, 190–195. [[CrossRef](#)]
62. van Dam, J.E. Natural fibres and the environment: Environmental benefits of natural fibre production and use. In Proceedings of the Symposium on Natural Fibres, Rome, Italy, 20 October 2008; pp. 3–17.
63. Spacilova, M.; Dytrych, P.; Lexa, M.; Wimmerova, L.; Masin, P.; Kvacek, R.; Solcova, O. An Innovative Sorption Technology for Removing Microplastics from Wastewater. *Water* **2023**, *15*, 892. [[CrossRef](#)]
64. Ha, T.T.; Viet, N.M.; Thanh, P.T.; Quan, V.T. Loofah plant—Derived biodegradable superhydrophobic sponge for effective removal of oil and microplastic from water. *Environ. Technol. Innov.* **2023**, *32*, 103265. [[CrossRef](#)]
65. Oliveira, A.C.; Neto, A.D.; Moura, M.C.; Dantas, T.C. Use of surfactant-modified adsorbents in the removal of microplastics from wastewater. *J. Environ. Chem. Eng.* **2023**, *11*, 110827. [[CrossRef](#)]
66. Fernández, V.; Khayet, M. Evaluation of the surface free energy of plant surfaces: Toward standardizing the procedure. *Front. Plant Sci.* **2015**, *6*, 145486. [[CrossRef](#)] [[PubMed](#)]
67. Ran, J.; Talebian-Kiakalaieh, A.; Zhang, S.; Hashem, E.; Guo, M.; Qiao, S. Recent advancement on photocatalytic plastic upcycling. *Chem. Sci.* **2024**, *15*, 1611–1637. [[CrossRef](#)]
68. Wang, L.; Jiang, S.; Gui, W.; Li, H.; Wu, J.; Wang, H.; Yang, J. Photocatalytic Upcycling of Plastic Waste: Mechanism, Integrating Modus, and Selectivity. *Small Struct.* **2023**, *4*, 2300142. [[CrossRef](#)]
69. Banik, H. Selected Properties of Cattail Fibre for Biomedical Applications. Master's Thesis, Department of Biosystems Engineering, University of Manitoba, Winnipeg, MB, Canada, 2022.
70. Chakma, K.; Cicek, N.; Rahman, M. Characterization of cattail fibre chemical groups by Fourier-Transform infrared Spectroscopy (FTIR). In *Proceedings of the Manitoba Institute of Materials (MIM) Annual Conference*; University of Manitoba: Winnipeg, MB, Canada, 2018.
71. Barragán, E.U.; Guerrero, C.F.; Zamudio, A.M.; Cepeda, A.B.; Heinze, T.; Koschella, A. Isolation of cellulose nanocrystals from *Typha domingensis* named southern cattail using a batch reactor. *Fibers Polym.* **2019**, *20*, 1136–1144. [[CrossRef](#)]
72. Nandiyanto, A.B.; Oktiani, R.; Ragadhita, R. How to read and interpret FTIR spectroscopy of organic material. *Indones. J. Sci. Technol.* **2019**, *7*, 97–118. [[CrossRef](#)]
73. Cao, S.; Dong, T.; Xu, G.; Wang, F. Study on structure and wetting characteristic of cattail fibers as natural materials for oil sorption. *Environ. Technol.* **2016**, *37*, 3193–3199. [[CrossRef](#)]
74. Bhuiyan, Z. The Effect of Scouring on Cattail Fibre Properties for Biomedical Applications. Master Academic Dissertation, University of Manitoba, Winnipeg, MB, Canada, 2019.
75. Dong, T.; Xu, G.; Wang, F. Oil spill cleanup by structured natural sorbents made from cattail fibers. *Ind. Crops Prod.* **2015**, *76*, 25–33. [[CrossRef](#)]
76. Cui, F.; Li, H.; Chen, C.; Wang, Z.; Liu, X.; Jiang, G.; Cheng, T.; Bai, R.; Song, L. Cattail fibers as source of cellulose to prepare a novel type of composite aerogel adsorbent for the removal of enrofloxacin in wastewater. *Int. J. Biol. Macromol.* **2021**, *191*, 171–181. [[CrossRef](#)] [[PubMed](#)]

77. Wu, S.; Zhang, J.; Li, C.; Wang, F.; Shi, L.; Tao, M.; Weng, B.; Yan, B.; Guo, Y.; Chen, Y. Characterization of potential cellulose fiber from cattail fiber: A study on micro/nano structure and other properties. *Int. J. Biol. Macromol.* **2021**, *193*, 27–37. [CrossRef] [PubMed]
78. Kamali Moghaddam, M. Typha leaves fiber and its composites: A review. *J. Nat. Fibers.* **2022**, *19*, 4993–5007. [CrossRef]
79. Kamali Moghaddam, M. Structural and thermal properties of cellulose microfibril isolated from *Typha australis* by sequential alkali-oxidative treatment. *J. Nat. Fibers.* **2022**, *19*, 10526–10538. [CrossRef]
80. Guechi, E.; Benabdesselam, S. Removal of cadmium and copper from aqueous media by biosorption on cattail (*Typha angustifolia*) leaves: Kinetic and isotherm studies. *Water Treat. Desalin.* **2020**, *173*, 367–382. [CrossRef]
81. MacFarlane, D.R.; Kar, M.; Pringle, J.M. *Fundamentals of Ionic Liquids: From Chemistry to Applications*; John Wiley & Sons: Weinheim, Germany, 2017; p. 250.
82. Al-Hakkak, J.S.; Barbooti, M.M. Thermogravimetric study on typha (*Typha angustifolia* L.). *J. Therm. Anal.* **1989**, *35*, 815–821. [CrossRef]
83. Sebio-Punal, T.; Naya, S.; López-Beceiro, J.; Tarrío-Saavedra, J.; Artiaga, R. Thermogravimetric analysis of wood, holocellulose, and lignin from five wood species. *J. Therm. Anal. Calorim.* **2012**, *109*, 1163–1167. [CrossRef]
84. Chakma, K.; Cicek, N.; Rahman, M. Fiber extraction efficiency, quality and characterization of cattail fibres for textile applications. In Proceedings of the Canadian Society for Bioengineering Conference (CSBE), Winnipeg, MB, Canada, 6–10 August 2017.
85. Ifeuebuegu, A.O.; Johnson, A. Nonconventional low-cost cellulose-and keratin-based biopolymeric sorbents for oil/water separation and spill cleanup: A review. *Crit. Rev. Environ. Sci. Technol.* **2017**, *47*, 964–1001. [CrossRef]
86. Schellbach, S.L.; Monteiro, S.N.; Drelich, J.W. A novel method for contact angle measurements on natural fibers. *Mater. Lett.* **2016**, *164*, 599–604. [CrossRef]
87. Accu Dyne TestTM. Critical Surface Tension and Contact Angle with Water for Various Polymers. Available online: https://www.accudynetest.com/polytable_03.html?sortby=contact_angle (accessed on 27 February 2024).
88. de Luna, M.S.; Galizia, M.; Wojnarowicz, J.; Rosa, R.; Lojkowski, W.; Leonelli, C.; Ancierno, D.; Filippone, G. Dispersing hydrophilic nanoparticles in hydrophobic polymers: HDPE/ZnO nanocomposites by a novel template-based approach. *eXPRESS Polym. Lett.* **2014**, *8*, 362–372. [CrossRef]
89. Siddiqui, A.J.; Chaudhury, K.; Adhikari, B. Hydrophilic low density polyethylene (LDPE) films for cell adhesion and proliferation. *Res. Rev. J. Med. Chem.* **2005**, *1*, 143–154.
90. Nieto, D.R.; Santese, F.; Toth, R.; Posocco, P.; Pricl, S.; Fermeglia, M. Simple, fast, and accurate in silico estimations of contact angle, surface tension, and work of adhesion of water and oil nanodroplets on amorphous polypropylene surfaces. *ACS Appl. Mater. Interfaces* **2012**, *4*, 2855–2859. [CrossRef] [PubMed]
91. Sant’Ana, P.L.; Bortoleto, J.R.; Drrant, S.F. Contact Angle and Wettability of Commercial Polymers after Plasma Treatment. *LJP* **2022**, *22*, 13–33.
92. Pesonen-Leinonen, E. Determination of Cleanability of Plastic Surfaces. PhD. Dissertation, Faculty of Agriculture and Forestry, University of Helsinki, Helsinki, Finland, 2005; pp. 1–67.
93. Biolin Scientific. Attension. Technology Note 7. Influence of Surface Roughness on Contact Angle and Wettability. Available online: <https://www.biolinscientific.com> (accessed on 27 February 2024).
94. Rahman, M.; Cicek, N.; Chakma, K. The optimum parameters for fibre yield (%) and characterization of *Typha latifolia* L. fibres for textile applications. *Fibers Polym.* **2021**, *22*, 1543–1555. [CrossRef]
95. Seo, Y.B.; Lee, M.W. Use of non-wood fibres (from cattails and red algae) and their effects on paper opacity. *Appita* **2011**, *64*, 445–449.
96. Wong, C.; McGowan, T.; Bajwa, S.G.; Bajwa, D.S. Impact of fiber treatment on the oil absorption characteristics of plant fibers. *BioResources* **2016**, *11*, 6452–6463. [CrossRef]
97. Wang, H.; Liu, C.; Shen, R.; Gao, J.; Li, J. An efficient approach to prepare water-redispersible starch nanocrystals from waxy potato starch. *Polymers* **2021**, *13*, 431. [CrossRef] [PubMed]
98. Sentharamaiah, P.; Kathiresan, M. Characterization of raw and alkali treated new natural cellulosic fiber from *Coccinia grandis*. *Carbohydr. Polym.* **2018**, *186*, 332–343. [CrossRef]
99. Mays, T.J. A new classification of pore sizes. *Stud. Surf. Sci. Catal.* **2007**, *160*, 57–62.
100. Vinayagam, V.; Murugan, S.; Kumaresan, R.; Narayanan, M.; Sillanpää, M.; Dai Viet, N.V.; Kushwaha, O.S.; Jenis, P.; Potdar, P.; Gadiya, S. Sustainable adsorbents for the removal of pharmaceuticals from wastewater: A review. *Chemosphere* **2022**, *300*, 134597. [CrossRef] [PubMed]
101. Lampman, S.; Bonnie Sanders, B.; Hrivnak, N.; Kinson, J.; Polakowski, C. *Characterization and Failure Analysis of Plastics*; ASM International: Cambridge, MA, USA, 2003.
102. Kent, R. *Energy Management in Plastics Processing: Strategies, Targets, Techniques, and Tools*; Elsevier: Cambridge, MA, USA, 2018; p. 441.
103. Chackalamannil, S.; Rotella, D.; Ward, S. (Eds.) *Comprehensive Medicinal Chemistry III*; Elsevier: Cambridge, MA, USA, 2017.
104. Letcher, T.M. *Storing Energy: With Special Reference to Renewable Energy Sources*; Elsevier: Cambridge, MA, USA, 2022.
105. Godwin, A.D.; Kutz, M. *Applied Plastics Engineering Handbook*; William Andrew Applied Science Publishers: Cambridge, MA, USA, 2017.

106. Tilton, R.D.; Robertson, C.R.; Gast, A.P. Manipulation of hydrophobic interactions in protein adsorption. *Langmuir* **1991**, *7*, 2710–2718. [[CrossRef](#)]
107. Puddu, V.; Perry, C.C. Peptide adsorption on silica nanoparticles: Evidence of hydrophobic interactions. *ACS Nano* **2012**, *6*, 6356–6363. [[CrossRef](#)] [[PubMed](#)]
108. Baldi, L.D.; Lamazaki, E.T.; Atvars, T.D. Evaluation of the polarity of polyamide surfaces using the fluorescence emission of pyrene. *Dyes Pigm.* **2008**, *76*, 669–676. [[CrossRef](#)]
109. Guo, S.; Zou, Z.; Chen, Y.; Long, X.; Liu, M.; Li, X.; Tan, J.; Chen, R. Synergistic effect of hydrogen bonding and π - π interaction for enhanced adsorption of rhodamine B from water using corn straw biochar. *Environ. Pollut.* **2023**, *320*, 121060. [[CrossRef](#)] [[PubMed](#)]
110. Arthur, J.D.; Langhus, B.G.; Patel, C. *Technical Summary of Oil & Gas Produced Water Treatment Technologies*; All Consulting, LLC.: Tulsa, OK, USA, 2005.
111. Garde, S. Hydrophobic interactions in context. *Nature* **2015**, *517*, 277–279. [[CrossRef](#)] [[PubMed](#)]
112. Anastopoulos, I.; Pashalidis, I.; Kayan, B.; Kalderis, D. Microplastics as carriers of hydrophilic pollutants in an aqueous environment. *J. Mol. Liq.* **2022**, *350*, 118182. [[CrossRef](#)]
113. Raza, N.; Ahmed, B.; Zohora, F.; Bakya, J.; Ahmed, S.; Ahmed, S.F.; Mofijur, M.; Chowdhury, A.A.; Almomani, F. Microplastics as carriers of toxic pollutants: Source, transport, and toxicological effects. *Environ. Pollut.* **2023**, *343*, 123190. [[CrossRef](#)] [[PubMed](#)]

Disclaimer/Publisher's Note: The statements, opinions and data contained in all publications are solely those of the individual author(s) and contributor(s) and not of MDPI and/or the editor(s). MDPI and/or the editor(s) disclaim responsibility for any injury to people or property resulting from any ideas, methods, instructions or products referred to in the content.